

A Control Theoretical Approach to Online Constrained Optimization [★]

Umberto Casti ^a, Nicola Bastianello ^b, Ruggero Carli ^a, Sandro Zampieri ^a

^a*Department of Information Engineering (DEI), University of Padova, Italy*

^b*School of Electrical Engineering and Computer Science and Digital Futures, KTH Royal Institute of Technology, Sweden*

Abstract

In this paper we focus on the solution of online problems with time-varying, linear equality and inequality constraints. Our approach is to design a novel online algorithm by leveraging the tools of control theory. In particular, for the case of equality constraints only, using robust control we design an online algorithm with asymptotic convergence to the optimal trajectory, differently from the alternatives that achieve non-zero tracking error. When also inequality constraints are present, we show how to modify the proposed algorithm to account for the wind-up induced by the nonnegativity constraints on the dual variables. We report numerical results that corroborate the theoretical analysis, and show how the proposed approach outperforms state-of-the-art algorithms both with equality and inequality constraints.

Key words: online optimization, constrained optimization, control theory, anti-windup

1 Introduction

Recent advances in technology have made *online optimization* problems increasingly relevant in a wide range of applications, *e.g.* control [23,25], signal processing [19,17,24], and machine learning [31,15,10]. Online problems are characterized by costs and constraints that change over time, mirroring changes in the dynamic environments that arise in these applications. The focus then shifts from solving a single problem (as in static optimization) to solving a sequence of problems *in real time*. Specifically, in this paper we are interested in online optimization problems with linear equality and inequality constraints

$$\begin{aligned} \mathbf{x}_k^* &= \arg \min_{\mathbf{x} \in \mathbb{R}^n} f_k(\mathbf{x}) \\ \text{s.t. } \mathbf{G}_k \mathbf{x} &= \mathbf{h}_k \quad \mathbf{G}'_k \mathbf{x} \leq \mathbf{h}'_k \end{aligned} \quad k \in \mathbb{N} \quad (1)$$

where consecutive cost functions and sets of constraints arrive every $T_s > 0$ seconds. In the following, we assume that each problem in (1) has a unique solution.

Drawing from [33], we can distinguish two approaches to online optimization: *unstructured* and *structured*. Unstructured algorithms are designed by applying static optimization methods (*e.g.* gradient descent-ascent) to each (static) problem in the sequence (1). The convergence of these algorithms has been analyzed in *e.g.* [15,31,19,17] for unconstrained problems, and [28,9,39] for constrained ones; see also the surveys [12,33]. However, straightforwardly repurposing static methods for an online scenario does not leverage in any way knowledge of the dynamic nature of these problems. And indeed, usual convergence analyses guarantee that the output of the online algorithm tracks the optimal trajectory $\{\mathbf{x}_k^*\}_{k \in \mathbb{N}}$ with only finite precision.

As a consequence, the alternative approach of structured methods has received increasing attention. “Structured” refers to the fact that the online algorithms are designed by incorporating information – a model – of the cost and constraints variability, with the goal of tracking $\{\mathbf{x}_k^*\}_{k \in \mathbb{N}}$ with improved precision. One widely studied class of structured methods is that of *prediction-correction* algorithms [36,34,16,22,2], which leverage a set of assumptions on the rate of change of (1) as a rudimentary model

[★] Corresponding author N. Bastianello.

This work was supported in part by the Italian Ministry of University and Research (2020–2023) through Research Project PRIN 2017 Advanced Network Control of Future Smart Grids

Email addresses: umberto.casti@phd.unipd.it (Umberto Casti), nicolba@kth.se (Nicola Bastianello), carlirug@dei.unipd.it (Ruggero Carli), zampi@dei.unipd.it (Sandro Zampieri).

to provably increase tracking precision. Recently, some of the authors have proposed a structured algorithm for unconstrained problems, which is designed using a fully fledged model of the cost function [3]. Accessing a detailed model of the problem allows us to draw from control theory to further improve tracking precision over previous algorithms. In this paper we focus on the control theoretical design of online algorithm, with the goal of extending it to solve constrained problems as well.

By taking this approach, we place our contribution at the productive intersection of control theory and optimization, both static and online. In particular, the design of optimization algorithms using control theoretical techniques has been explored in [21,37,38,26,18,27] for static optimization, and [29,30,35,13] for online optimization. In particular, [29,30] exploit a linear model for the evolution of $\{\mathbf{x}_k^*\}_{k \in \mathbb{N}}$ to analyze convergence of online algorithms, [35] leverages Kalman-filtering for *stochastic* online optimization, and [13] uses contraction analysis to design and analyze continuous-time online algorithms. In turn, online optimization has also been used extensively as a tool to design controllers, giving rise to *feedback optimization*. As the name suggests, in feedback optimization an online optimization algorithm is connected in a feedback loop with a dynamical system [6,11,20], as in the model predictive control (MPC) set-up [23]. Specifically, the output of the algorithm serves as control input to the system, whose output in turn acts on the online problem formulation.

We are now ready to discuss the proposed contribution. As mentioned above, we focus on the solution of online problems with linear equality and inequality constraints, cf. (1). In particular, the goal is to extend the (structured) control theoretical approach of [3] to handle these problems. The key to this approach is interpreting the online problem as the plant, for which we have a model, that needs to be controlled. We start our development by working on quadratic online problems with linear equality constraints, which are relevant in and of themselves in signal processing and machine learning [15,31]. This class of problems can be reformulated as *linear control problems with uncertainties*, which allows us to design a novel online algorithm by leveraging the internal model principle and techniques from robust control, as well as linear algebra results on saddle matrices. The proposed algorithms can then be shown to achieve *zero* tracking error, differently from unstructured methods and alternative structured ones. However, the proposed algorithm cannot be applied in a straightforward manner when also inequality constraints are present. Indeed, these constraints translate into non-negativity constraints on the dual variables, and the problem cannot be cast as a linear control problem. But by noticing that non-negativity constraints act as a *saturation*, we are able to incorporate them in the algorithm with the use of an *anti wind-up* technique. We conclude the paper with numerical results that compare the proposed algorithm to alterna-

tive methods, showing its promising performance when both equality and inequality constraints are present. To summarize, we offer the following contributions:

- (1) We take a control theoretical approach to design online algorithms for problems with linear equality and inequality constraints. In particular, when the cost is quadratic and only equality constraints are present, we show how a zero tracking error can be achieved.
- (2) We extend the proposed algorithm to deal with inequality constraints as well, by leveraging an anti wind-up mechanism.
- (3) We present numerical simulations to show how the proposed algorithms can outperform alternative unstructured methods, both with equality and inequality constraints, and both for quadratic and non-quadratic costs.

2 Problem formulation and background

Notation. We denote by \mathbb{N} , \mathbb{R} the natural and real numbers, respectively, and by $\mathbb{R}[z]$, $\mathbb{R}(z)$ the set of polynomials and of rational functions in z with real coefficients. Vectors and matrices are denoted by bold letters, *e.g.* $\mathbf{x} \in \mathbb{R}^n$ and $\mathbf{A} \in \mathbb{R}^{n \times n}$. The symbol \mathbf{I} denotes the identity, $\mathbf{1}$ denotes the vector of all 1s and $\mathbf{0}$ denotes the vector of all 0s. The 2-norm of a vector and the induced 2-norm of a matrix are both denoted by $\|\cdot\|$. Moreover, in the following, the entry-wise partial order in \mathbb{R}^n is considered. Therefore, the notation $\mathbf{x} \leq \mathbf{y}$ denotes the fact that the inequality holds for every pair of corresponding entries in \mathbf{x} and \mathbf{y} . The symbol $\mathbf{A} \succeq \mathbf{B}$ (or $\mathbf{A} \succ \mathbf{B}$) means that the matrix $\mathbf{A} - \mathbf{B}$ is positive semi-definite (or positive definite). \otimes denotes the Kronecker product and diag denotes a (block) diagonal matrix built from the arguments. For a function $f(\mathbf{x})$ from \mathbb{R}^n to \mathbb{R} , we denote by ∇f its gradient while for a function $f(\mathbf{x}, \mathbf{w})$ from $\mathbb{R}^n \times \mathbb{R}^m$ to \mathbb{R} , we denote $\nabla_{\mathbf{x}} f(\mathbf{x}, \mathbf{w})$ and $\nabla_{\mathbf{w}} f(\mathbf{x}, \mathbf{w})$ its gradient with respect to \mathbf{x} and \mathbf{w} , respectively. $f(\mathbf{x})$ is λ -strongly convex, $\lambda > 0$, iff $f(\mathbf{x}) - \frac{\lambda}{2} \|\mathbf{x}\|^2$ is convex, and $\bar{\lambda}$ -smooth iff $\nabla f(\mathbf{x})$ is $\bar{\lambda}$ -Lipschitz continuous. Given a symmetric matrix \mathbf{A} , with $\lambda(\mathbf{A})$ and $\bar{\lambda}(\mathbf{A})$ we denote the minimum and the maximum eigenvalue of \mathbf{A} , respectively, while for any matrix \mathbf{B} with $\sigma(\mathbf{B})$ and $\bar{\sigma}(\mathbf{B})$ we denote the minimum and the maximum singular value of \mathbf{B} . Moreover with $\kappa(\mathbf{B})$ we denote the condition number on \mathbf{B} . Finally, $\text{proj}_{\geq 0}(\cdot) : \mathbb{R}^n \rightarrow \mathbb{R}_{\geq 0}^n$ represents the function that returns the closest element (in Euclidean norm) in the non-negative orthant. Finally, we denote by $\mathcal{Z}[\cdot]$ the \mathcal{Z} -transform of a given signal.

2.1 Problem formulation

We begin by focusing on a specific sub-class of (1), that is, *quadratic, linearly constrained, online* problems of the

following form:

$$\begin{aligned} \mathbf{x}_k^* &= \arg \min_{\mathbf{x} \in \mathbb{R}^n} f_k(\mathbf{x}) \\ \text{s.t. } \mathbf{G}\mathbf{x} &= \mathbf{h}_k \quad k \in \mathbb{N}. \\ \mathbf{G}'\mathbf{x} &\leq \mathbf{h}'_k \end{aligned} \quad (2)$$

where $\mathbf{x} \in \mathbb{R}^n$, $f_k(\mathbf{x}) := \frac{1}{2}\mathbf{x}^\top \mathbf{A}\mathbf{x} + \mathbf{b}_k^\top \mathbf{x}$ and $\mathbf{A} \in \mathbb{R}^{n \times n}$, $\mathbf{G} \in \mathbb{R}^{p \times n}$ and $\mathbf{G}' \in \mathbb{R}^{p' \times n}$ are fixed matrices, while $\mathbf{b}_k \in \mathbb{R}^n$, $\mathbf{h}_k \in \mathbb{R}^p$ and $\mathbf{h}'_k \in \mathbb{R}^{p'}$ are time-varying. We make the following assumptions.

Assumption 1 (Strongly convex and smooth)

The symmetric matrix \mathbf{A} is such that

$$\lambda \mathbf{I} \preceq \mathbf{A} \preceq \bar{\lambda} \mathbf{I}, \quad (3)$$

with $0 < \lambda \leq \bar{\lambda} \leq +\infty$. This is equivalent to imposing that the cost functions $\{f_k\}_{k \in \mathbb{N}}$ are λ -strongly convex and $\bar{\lambda}$ -smooth for any time $k \in \mathbb{N}$.

Assumption 2 (Constraints) (i) The constraint matrix $[\mathbf{G}^\top \mid \mathbf{G}'^\top]^\top \in \mathbb{R}^{(p+p') \times n}$ is full row rank. (ii) The symmetric matrix $\mathbf{G}\mathbf{A}^{-1}\mathbf{G}^\top$ is such that

$$\mu \mathbf{I} \preceq \mathbf{G}\mathbf{A}^{-1}\mathbf{G}^\top \preceq \bar{\mu} \mathbf{I}, \quad (4)$$

with $0 < \mu \leq \bar{\mu} \leq +\infty$.

Assumptions 1 and 2, imply that each problem in (2) has a unique minimizer, and we can define the optimal trajectory $\{\mathbf{x}_k^*\}_{k \in \mathbb{N}}$. In particular, Assumption 1 is widely used in online optimization [12], since the strong convexity of the cost implies that, at any $k \in \mathbb{N}$, there is a unique primal solution \mathbf{x}^* . Moreover, Assumption 2 (i) guarantees that also the dual solution is unique [8, p. 523].

Remark 3 In the following, we assume that the online algorithm only has access to an oracle for the gradient. Moreover, we assume that in the design of this algorithm we can use only the values λ , $\bar{\lambda}$, μ and $\bar{\mu}$ appearing in (3) and (4). This assumption is made to align with gradient methods that our technique aims to improve, where the algorithm does not need to possess full knowledge of \mathbf{A} and \mathbf{G} . Concerning the bound (4) on $\mathbf{G}\mathbf{A}^{-1}\mathbf{G}^\top$ notice that the values of μ and $\bar{\mu}$ can be obtained from λ , $\bar{\lambda}$ and from bounds on the singular values of \mathbf{G} . Indeed, observe that

$$\frac{\sigma^2(\mathbf{G})}{\bar{\lambda}(\mathbf{A})} \leq \lambda(\mathbf{G}\mathbf{A}^{-1}\mathbf{G}^\top) \leq \bar{\lambda}(\mathbf{G}\mathbf{A}^{-1}\mathbf{G}^\top) \leq \frac{\bar{\sigma}^2(\mathbf{G})}{\lambda(\mathbf{A})}. \quad (5)$$

Our objective is to design an online algorithm that can track the optimizer sequence $\{\mathbf{x}_k^*\}_{k \in \mathbb{N}}$ in a real-time fashion. Let $\{\mathbf{x}_k\}_{k \in \mathbb{N}}$ be the output of such an algorithm.

The goal is to ensure that

$$\limsup_{k \rightarrow \infty} \|\mathbf{x}_k - \mathbf{x}_k^*\| \leq B < \infty. \quad (6)$$

Notice how the dynamic nature of the problem, imposes an important limitation on the algorithm, as it needs to compute the next output \mathbf{x}_k within the time interval between the arrival of f_{k-1} and f_k , namely $[(k-1)T_s, kT_s)$.

As discussed in section 1, in this paper we focus on a *control theoretical* approach to designing online algorithms that can achieve (6). We start our development by focusing on problems with equality constraints only, for which we propose a novel algorithm in section 3, and analyze its convergence. In section 4 we then extend the applicability of the algorithm to inequality constraints as well, by leveraging anti wind-up techniques.

3 Online Optimization with Equality Constraints

In this section we will analyze Problem (2) with only equality constraints, namely we will study the following problem:

$$\begin{aligned} \mathbf{x}_k^* &= \arg \min_{\mathbf{x} \in \mathbb{R}^n} f_k(\mathbf{x}) \\ \text{s.t. } \mathbf{G}\mathbf{x} &= \mathbf{h}_k \quad k \in \mathbb{N}, \end{aligned} \quad (7)$$

where $f_k(\mathbf{x}) := \frac{1}{2}\mathbf{x}^\top \mathbf{A}\mathbf{x} + \mathbf{b}_k^\top \mathbf{x}$. We also suppose that we have a partial knowledge on the time-varying terms, as clarified by the following assumption.

Assumption 4 (Models of \mathbf{b}_k and \mathbf{h}_k) The sequence of vectors $\{\mathbf{b}_k\}_{k \in \mathbb{N}}$ and $\{\mathbf{h}_k\}_{k \in \mathbb{N}}$ have rational \mathcal{Z} -transforms

$$\begin{aligned} \hat{\mathbf{b}}(z) &:= \mathcal{Z}[\mathbf{b}_k] = \frac{\mathbf{b}_N(z)}{p(z)}, \\ \hat{\mathbf{h}}(z) &:= \mathcal{Z}[\mathbf{h}_k] = \frac{\mathbf{h}_N(z)}{p(z)}, \end{aligned} \quad (8)$$

where the polynomial $p(z) = z^m + \sum_{i=0}^{m-1} p_i z^i$ is known and whose zeros are assumed to be all marginally unstable¹. The numerators, $\mathbf{b}_N(z)$ and $\mathbf{h}_N(z)$, are instead assumed to be unknown.

Remark 5 Observe that imposing the same polynomial at the denominator on the rational \mathcal{Z} -transforms in Equation (8) is not restrictive. In fact, if this is not the case, it is always possible to choose the least common multiple of the denominators. Moreover, also the

¹ A zero $\bar{z} \in \mathbb{C}$ of a polynomial is said to be marginally unstable if $|\bar{z}| = 1$.

assumption that all the zeros of $p(z)$ are marginally unstable is not restrictive, as it is easy to extend the proposed methods to general polynomials only at the cost of a more complicated notation.

Taking inspiration from [3], we develop an algorithm based on the *primal-dual* problem that leverages the Internal Model Principle to address Problem (7). In this case, we are able to provide precise and rigorous proof of the algorithm convergence.

3.1 The design of the algorithm

In this section we extend the model-based approach proposed in [3] to address the constrained problem (7). To this aim, we define the time-varying Lagrangian

$$\mathcal{L}_k(\mathbf{x}, \mathbf{w}) = f_k(\mathbf{x}) + \mathbf{w}^\top (\mathbf{G}\mathbf{x} - \mathbf{h}_k), \quad k \in \mathbb{N}, \quad (9)$$

where $\mathbf{w} \in \mathbb{R}^p$ represents the Lagrange multiplier. The solution of the *primal-dual* problem [8, p. 244] is given by the pair of vectors $\mathbf{x}_k^* \in \mathbb{R}^n$ and $\mathbf{w}_k^* \in \mathbb{R}^p$ satisfying the equation

$$\begin{bmatrix} \mathbf{e}_k \\ \mathbf{f}_k \end{bmatrix} := \begin{bmatrix} \nabla_{\mathbf{x}} \mathcal{L}_k(\mathbf{x}_k, \mathbf{w}_k) \\ \nabla_{\mathbf{w}} \mathcal{L}_k(\mathbf{x}_k, \mathbf{w}_k) \end{bmatrix} = \begin{bmatrix} \mathbf{0} \\ \mathbf{0} \end{bmatrix}, \quad (10)$$

where, in our case,

$$\begin{aligned} \nabla_{\mathbf{x}} \mathcal{L}_k(\mathbf{x}_k, \mathbf{w}_k) &= \mathbf{A}\mathbf{x}_k + \mathbf{b}_k + \mathbf{G}^\top \mathbf{w}_k, \\ \nabla_{\mathbf{w}} \mathcal{L}_k(\mathbf{x}_k, \mathbf{w}_k) &= \mathbf{G}\mathbf{x}_k - \mathbf{h}_k. \end{aligned} \quad (11)$$

A commonly employed algorithm for solving a convex problem with linear equality constraints is based on the gradient *descent-ascent* of the *primal-dual* problem [7]. The natural extension of this *primal-dual* algorithm to the online setting yields the following iterations (cf. [6])

$$\begin{aligned} \mathbf{x}_{k+1} &= \mathbf{x}_k - \alpha \nabla_{\mathbf{x}_k} \mathcal{L}_k(\mathbf{x}_k, \mathbf{w}_k), \\ \mathbf{w}_{k+1} &= \mathbf{w}_k + \beta \nabla_{\mathbf{w}_k} \mathcal{L}_k(\mathbf{x}_k, \mathbf{w}_k), \end{aligned} \quad (12)$$

where $k \in \mathbb{N}$, and α and β are two positive parameters. Under Assumption 4, we can establish that the asymptotic tracking error $\|\mathbf{x}_k - \mathbf{x}_k^*\|$ is bounded. However, this asymptotic tracking error is not zero in general [6].

On the other hand resorting to the control scheme illustrated in Figure 1, we can obtain an algorithm able to find all the points where (10) is satisfied. The objective, therefore, is to design the transfer matrix,

$$\mathbf{C}(z) = \begin{bmatrix} \mathbf{C}_{11}(z) & \mathbf{C}_{12}(z) \\ \mathbf{C}_{21}(z) & \mathbf{C}_{22}(z) \end{bmatrix} \in \mathbb{R}^{(n+p) \times (n+p)}(z), \quad (13)$$

of the controller able to drive the signals \mathbf{e}_k and \mathbf{f}_k to zero.

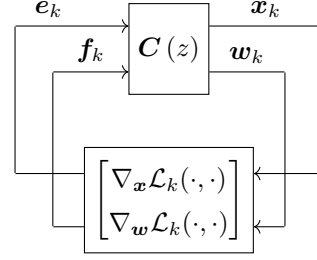


Fig. 1. The control scheme for the solution of (7).

Remark 6 A common alternative to the *primal-dual* algorithm in (12) is the *dual-ascent* algorithm where, in the update of \mathbf{w}_{k+1} , \mathbf{x}_{k+1} is used in place of \mathbf{x}_k . In general, the performances of the *dual-ascent* algorithm are similar to the ones of the *primal-dual* algorithm. For this reason, in this paper, we decided to compare our novel strategy only with the *primal-dual* algorithm.

3.2 Internal Model

Let us define the following \mathcal{Z} -transforms

$$\begin{aligned} \hat{\mathbf{x}}(z) &:= \mathcal{Z}[\mathbf{x}_k], \\ \hat{\mathbf{w}}(z) &:= \mathcal{Z}[\mathbf{w}_k], \\ \hat{\mathbf{e}}(z) &:= \mathcal{Z}[\mathbf{e}_k], \\ \hat{\mathbf{f}}(z) &:= \mathcal{Z}[\mathbf{f}_k]. \end{aligned}$$

By referring to the control scheme shown in Figure 1 we argue that

$$\begin{bmatrix} \hat{\mathbf{x}}(z) \\ \hat{\mathbf{w}}(z) \end{bmatrix} = \mathbf{C}(z) \begin{bmatrix} \hat{\mathbf{e}}(z) \\ \hat{\mathbf{f}}(z) \end{bmatrix}. \quad (14)$$

From Equation (11) we also have that

$$\begin{aligned} \begin{bmatrix} \hat{\mathbf{e}}(z) \\ \hat{\mathbf{f}}(z) \end{bmatrix} &= \underbrace{\begin{bmatrix} \mathbf{A} & \mathbf{G}^\top \\ \mathbf{G} & \mathbf{0}_{p \times p} \end{bmatrix}}_{:=\mathcal{A}} \begin{bmatrix} \hat{\mathbf{x}}(z) \\ \hat{\mathbf{w}}(z) \end{bmatrix} + \begin{bmatrix} \hat{\mathbf{b}}(z) \\ -\hat{\mathbf{h}}(z) \end{bmatrix} \\ &= \mathcal{A}\mathbf{C}(z) \begin{bmatrix} \hat{\mathbf{e}}(z) \\ \hat{\mathbf{f}}(z) \end{bmatrix} + \begin{bmatrix} \hat{\mathbf{b}}(z) \\ -\hat{\mathbf{h}}(z) \end{bmatrix}, \end{aligned}$$

where $\mathcal{A} \in \mathbb{R}^{(n+p) \times (n+p)}$. In this way we obtain

$$\begin{bmatrix} \hat{\mathbf{e}}(z) \\ \hat{\mathbf{f}}(z) \end{bmatrix} = [\mathbf{I} - \mathcal{A}\mathbf{C}(z)]^{-1} \begin{bmatrix} \hat{\mathbf{b}}(z) \\ -\hat{\mathbf{h}}(z) \end{bmatrix}. \quad (15)$$

We remark that \mathcal{A} is a so-called *saddle matrix* [4,5], and in the following we will leverage results for this class of matrices to design a suitable controller. Observe that from Assumption 4 we know that $\hat{\mathbf{b}}(z)$, $\hat{\mathbf{h}}(z)$ are rational

and hence $\hat{\mathbf{e}}(z), \hat{\mathbf{f}}(z)$ are rational as well. Therefore, if we prove that their poles are stable, namely inside the unit circle, than we can argue that the signals $\mathbf{e}_k, \mathbf{f}_k$ converge to zero, namely

$$\begin{bmatrix} \mathbf{e}_k \\ \mathbf{f}_k \end{bmatrix} \xrightarrow{k \rightarrow \infty} \begin{bmatrix} \mathbf{0} \\ \mathbf{0} \end{bmatrix}.$$

By applying the Internal Model Principle, the first step is to choose the controller $\mathbf{C}(z)$ able to cancel out the unstable poles of $\hat{\mathbf{b}}(z), \hat{\mathbf{h}}(z)$ that are the unstable zeros of $p(z)$ introduced in Assumption 4. Since we assumed that all the zeros of $p(z)$ are marginally unstable, then to this aim it is enough to choose

$$\mathbf{C}(z) = \frac{\mathbf{C}_N(z)}{p(z)},$$

where $\mathbf{C}_N(z) \in \mathbb{R}^{(n+p) \times (n+p)}[z]$ is a polynomial matrix. Indeed, this choice yields

$$\begin{bmatrix} \hat{\mathbf{e}}(z) \\ \hat{\mathbf{f}}(z) \end{bmatrix} = [p(z)\mathbf{I} - \mathcal{A}\mathbf{C}_N(z)]^{-1} \begin{bmatrix} \mathbf{b}_N(z) \\ -\mathbf{h}_N(z) \end{bmatrix}. \quad (16)$$

Then the poles of $\hat{\mathbf{e}}(z), \hat{\mathbf{f}}(z)$ coincide with the poles $[p(z)\mathbf{I} - \mathcal{A}\mathbf{C}_N(z)]^{-1}$ and so the goal is to determine $\mathbf{C}_N(z)$ such that all the poles of $[p(z)\mathbf{I} - \mathcal{A}\mathbf{C}_N(z)]^{-1}$ are stable.

3.3 Stabilizing controller

Observe that the matrix \mathcal{A} is in general indefinite, which implies that the control design approach proposed in [3] cannot be directly applied in our context. So we have to resort to a controller $\mathbf{C}_N(z)$ with a more general structure. Until now, we have considered a controller without a particular structure. Even though imposing a structure can limit the performance of the algorithms that can be obtained, the synthesis of general controllers can be complex and intractable. For that reason, we introduce a more structured version of the controller in which we impose that

$$\mathbf{C}_N(z) = c(z) \begin{bmatrix} \mathbf{I} & \mathbf{0} \\ \mathbf{0} & -\tau\mathbf{I} \end{bmatrix}, \quad (17)$$

where $c(z) = \sum_{i=0}^{m-1} c_i z^i \in \mathbb{R}[z]$ is a scalar polynomial of degree $m-1$ able to ensure strict properness of the controller transfer matrix, and τ is a positive parameter. Through this strategy we will see that it is possible to transform the design from a matrix to a scalar problem. With this choice of the controller we have that

$$[p(z)\mathbf{I} - \mathcal{A}\mathbf{C}_N(z)]^{-1} = [p(z)\mathbf{I} - c(z)\tilde{\mathcal{A}}(\tau)]^{-1}, \quad (18)$$

where

$$\tilde{\mathcal{A}}(\tau) = \mathcal{A} \begin{bmatrix} \mathbf{I} & \mathbf{0} \\ \mathbf{0} & -\tau\mathbf{I} \end{bmatrix} = \begin{bmatrix} \mathbf{A} & -\tau\mathbf{G}^\top \\ \mathbf{G} & \mathbf{0} \end{bmatrix}. \quad (19)$$

We will see that the application of robust control techniques, needed in the proposed design method, is simpler if we impose that the matrix $\tilde{\mathcal{A}}(\tau)$ has real and positive eigenvalues. The control structure described in (17) is able to guarantee this condition.

Remark 7 *The controller structure in Equation (17) can, in principle, be generalized to*

$$\mathbf{C}_N(z) = c(z) \begin{bmatrix} \alpha\mathbf{I} & \mathbf{0} \\ \mathbf{0} & -\beta\mathbf{I} \end{bmatrix},$$

where $\alpha, \beta > 0$. This controller can be transformed to

$$\mathbf{C}_N(z) = \underbrace{c(z)\alpha}_{:=\tilde{c}(z)} \begin{bmatrix} \mathbf{I} & \mathbf{0} \\ \mathbf{0} & -\frac{\beta}{\alpha}\mathbf{I} \end{bmatrix}.$$

Since $c(z)$ is a polynomial that needs to be designed, we can always incorporate the extra degree of freedom α in it.

With respect to the analysis done in [3], the design the polynomial $c(z)$ able to make all the poles of (18) stable has the additional issue that matrix $\tilde{\mathcal{A}}(\tau)$ is not always diagonalizable. Consequently, we will approach the problem using a slightly different strategy.

Consider the Schur decomposition of $\tilde{\mathcal{A}}(\tau)$, given by $\tilde{\mathcal{A}}(\tau) = \mathbf{Q}\mathbf{U}\mathbf{Q}^\top$, where \mathbf{Q} is a unitary matrix and \mathbf{U} is an upper triangular matrix. By substituting this decomposition in (18) we obtain

$$\begin{aligned} [p(z)\mathbf{I} - c(z)\tilde{\mathcal{A}}(\tau)]^{-1} &= \\ &= \mathbf{Q} [p(z)\mathbf{I} - c(z)\mathbf{U}]^{-1} \mathbf{Q}^\top. \end{aligned} \quad (20)$$

Hence the poles of $[p(z)\mathbf{I} - \mathcal{A}\mathbf{C}_N(z)]^{-1}$ coincide with the poles of $[p(z)\mathbf{I} - c(z)\mathbf{U}]^{-1}$. Since the (i, j) element of this matrix has the following form

$$\begin{aligned} ([p(z)\mathbf{I} - c(z)\mathbf{U}]^{-1})_{ij} &= \\ &= \frac{(\text{adj}[p(z)\mathbf{I} - c(z)\mathbf{U}])_{ij}}{\det[p(z)\mathbf{I} - c(z)\mathbf{U}]}. \end{aligned} \quad (21)$$

then the poles of this matrix are surely zeros of the polynomial $\det[p(z)\mathbf{I} - c(z)\mathbf{U}]$. The triangular form of \mathbf{U}

implies that the set of these zeros coincides with the union of the zeros of the polynomials

$$p(z) - c(z) \lambda_i \quad (22)$$

where $\lambda_i, i = 1, \dots, n$, are all the eigenvalues of $\tilde{\mathcal{A}}(\tau)$.

As emphasized in Remark 3, our knowledge of the eigenvalues of \mathbf{A} , and consequently also of $\tilde{\mathcal{A}}(\tau)$, is incomplete. Therefore, we need to employ a robust control technique capable to obtain stabilizing controllers of a uncertain systems. In this regard, we rely on the findings of [14], which employed an LMI-based approach to address this issue.

To devise a robust controller for this problem, it is essential to obtain an estimate of the eigenvalues of the matrix $\tilde{\mathcal{A}}(\tau)$. These eigenvalues are contingent upon the specific matrices \mathbf{A} and \mathbf{G} , as well as the parameter τ . The following lemma then provides bounds for the eigenvalues of $\tilde{\mathcal{A}}(\tau)$, and is proved by exploiting the fact that $\tilde{\mathcal{A}}(\tau)$ is a post-conditioned saddle matrix [4,5].

Lemma 8 (Eigenvalues of $\tilde{\mathcal{A}}(\tau)$) *Given $\tilde{\mathcal{A}}(\tau)$ as in (19), if τ is such that*

$$0 < \tau \leq \tau^* := \frac{\lambda(\mathbf{A})}{4\bar{\lambda}(\mathbf{G}\mathbf{A}^{-1}\mathbf{G}^\top)}. \quad (23)$$

then the eigenvalues of $\tilde{\mathcal{A}}(\tau)$ are real and belong to the following interval

$$[\tau\lambda(\mathbf{G}\mathbf{A}^{-1}\mathbf{G}^\top), \bar{\lambda}(\mathbf{A})] \quad (24)$$

PROOF. As proved in [5, Corollary 2.7] if $\lambda(\mathbf{A}) \geq 4\tau\bar{\lambda}(\mathbf{G}\mathbf{A}^{-1}\mathbf{G}^\top)$, then $\tilde{\mathcal{A}}(\tau)$ has all real eigenvalues, which implies inequality (23) and this implies that $\tilde{\mathcal{A}}(\tau)$ has all real eigenvalues. Moreover, thanks to the fact that \mathbf{G} is full row rank and using [5, Proposition 2.12] and [32, Theorem 2.1] we know that the eigenvalues of $\tilde{\mathcal{A}}(\tau)$ belongs to the interval

$$[\min\{\lambda(\mathbf{A}), \tau\lambda(\mathbf{G}\mathbf{A}^{-1}\mathbf{G}^\top)\}, \bar{\lambda}(\mathbf{A})]$$

Observe finally that, using (23) we can argue that

$$\begin{aligned} \tau\lambda(\mathbf{G}\mathbf{A}^{-1}\mathbf{G}^\top) &\leq \frac{\lambda(\mathbf{A})}{4\bar{\lambda}(\mathbf{G}\mathbf{A}^{-1}\mathbf{G}^\top)}\lambda(\mathbf{G}\mathbf{A}^{-1}\mathbf{G}^\top) \\ &= \frac{\lambda(\mathbf{A})}{4\kappa(\mathbf{G}\mathbf{A}^{-1}\mathbf{G}^\top)} \leq \lambda(\mathbf{A}), \end{aligned} \quad (25)$$

which yields (24). \square

Based on Lemma 8, we can determine τ such that the eigenvalues of $\tilde{\mathcal{A}}(\tau)$ are real and fall in the interval specified in Equation (24). To stabilize the polynomials given by Equation (22), it is sufficient to select an appropriate $c(z)$ that stabilizes the polynomials

$$p(z) - c(z) \lambda, \quad (26)$$

for all $\lambda \in [\lambda(\tilde{\mathcal{A}}(\tau)), \bar{\lambda}(\tilde{\mathcal{A}}(\tau))]$. But requiring the stability of the polynomials in (26) coincides with requiring the stability of the associated companion matrices $\mathbf{F}_c(\lambda) := \mathbf{F} + \lambda\mathbf{C}\mathbf{K}$, where

$$\mathbf{F} = \begin{bmatrix} 0 & 1 & 0 & \dots & 0 \\ \vdots & \vdots & \vdots & \ddots & \vdots \\ \vdots & \vdots & \vdots & \ddots & 0 \\ 0 & \dots & \dots & \dots & 1 \\ -p_0 & \dots & \dots & \dots & -p_{m-1} \end{bmatrix} \quad \mathbf{C} = \begin{bmatrix} 0 \\ \vdots \\ \vdots \\ 0 \\ 1 \end{bmatrix} \quad (27)$$

$$\mathbf{K} = [c_0 \dots \dots \dots c_{m-1}] \quad .$$

By denoting $\underline{\lambda} := \lambda(\tilde{\mathcal{A}}(\tau))$ and $\bar{\lambda} := \bar{\lambda}(\tilde{\mathcal{A}}(\tau))$, we can express λ as a convex combination of these two extreme values using the equation:

$$\lambda = \alpha(\lambda)\underline{\lambda} + (1 - \alpha(\lambda))\bar{\lambda}, \quad \alpha(\lambda) = \frac{\bar{\lambda} - \lambda}{\bar{\lambda} - \underline{\lambda}}$$

With this expression, we can apply the following result [14, Theorem 3]), and subsequently derive the polynomial $c(z)$ by solving the two LMIs of size m in the following lemma.

Lemma 9 (Stabilizing controller design) *The matrix $\mathbf{F}_c(\lambda)$ is asymptotically stable for any $\lambda \in [\underline{\lambda}, \bar{\lambda}]$ if there exist symmetric matrices $\underline{\mathbf{P}}, \bar{\mathbf{P}} \succ 0$, a square matrix $\mathbf{Q} \in \mathbb{R}^{m \times m}$, and a row vector $\mathbf{R} \in \mathbb{R}^{1 \times m}$ such that*

$$\begin{bmatrix} \underline{\mathbf{P}} & \mathbf{F}\mathbf{Q} + \underline{\mathbf{L}}\mathbf{C}\mathbf{R} \\ \mathbf{Q}^\top \mathbf{F}^\top + \underline{\mathbf{L}}\mathbf{R}^\top \mathbf{C}^\top & \mathbf{Q} + \mathbf{Q}^\top - \underline{\mathbf{P}} \end{bmatrix} \succ 0,$$

$$\begin{bmatrix} \bar{\mathbf{P}} & \mathbf{F}\mathbf{Q} + \bar{\mathbf{L}}\mathbf{C}\mathbf{R} \\ \mathbf{Q}^\top \mathbf{F}^\top + \bar{\mathbf{L}}\mathbf{R}^\top \mathbf{C}^\top & \mathbf{Q} + \mathbf{Q}^\top - \bar{\mathbf{P}} \end{bmatrix} \succ 0.$$

A stabilizing controller is then $\mathbf{K} = \mathbf{R}\mathbf{Q}^{-1}$.

These LMIs depend on the minimum and maximum eigenvalues of $\tilde{\mathcal{A}}(\tau)$. But, using Lemma 8, we can obtain the polynomial $c(z)$ by solving the two LMIs on the extremes of the interval in (24).

The feasibility of aforementioned robust control design procedure, based on [14, Theorem 3] depends on the ratio between the extremes of the interval. Precisely the possibility of obtaining a solution increases as much as this ratio get closer to one. Hence the best choice of the parameter τ is the maximum value ensuring that the eigenvalues of $\tilde{\mathcal{A}}(\tau)$ are real. From Lemma 8 this is $\tau = \tau^*$ and in this case we can argue that the eigenvalues of $\tilde{\mathcal{A}}(\tau^*)$ belong to the interval

$$\left[\frac{\lambda(\mathbf{A}) \lambda(\mathbf{G}\mathbf{A}^{-1}\mathbf{G}^\top)}{4\bar{\lambda}(\mathbf{G}\mathbf{A}^{-1}\mathbf{G}^\top)}, \bar{\lambda}(\mathbf{A}) \right],$$

and that the ratio between the extremes of this interval is

$$4\kappa(\mathbf{A}) \kappa(\mathbf{G}\mathbf{A}^{-1}\mathbf{G}^\top).$$

In case only the bounds given in Equations (3) and (4) are available, we choose

$$\tau = \tau_{\text{est}}^* := \frac{\lambda}{4\bar{\mu}}.$$

In this case we can argue that the eigenvalues of $\tilde{\mathcal{A}}(\tau_{\text{est}}^*)$ belong to the interval

$$\left[\frac{\lambda\bar{\mu}}{4\bar{\mu}}, \bar{\lambda} \right], \quad (28)$$

and the ratio between the extremes of this interval is

$$4\frac{\bar{\lambda}\bar{\mu}}{\lambda\bar{\mu}}. \quad (29)$$

3.4 The online algorithm

The algorithm consists in the translation in the time domain of the relations between the signals \mathbf{e}_k , \mathbf{f}_k , \mathbf{x}_k and \mathbf{w}_k that in the \mathcal{Z} -transform domain are given by

$$\hat{\mathbf{x}}(z) = \frac{c(z)}{p(z)} \hat{\mathbf{e}}(z), \quad \hat{\mathbf{w}}(z) = -\tau \frac{c(z)}{p(z)} \hat{\mathbf{f}}(z).$$

A state space realization of such relation is given by

$$\mathbf{z}_{k+1} = (\mathbf{F} \otimes \mathbf{I}) \mathbf{z}_k + (\mathbf{C} \otimes \mathbf{I}) \mathbf{e}_k \quad (30a)$$

$$\mathbf{y}_{k+1} = (\mathbf{F} \otimes \mathbf{I}) \mathbf{y}_k + (\mathbf{C} \otimes \mathbf{I}) \mathbf{f}_k \quad (30b)$$

$$\mathbf{x}_{k+1} = (\mathbf{K} \otimes \mathbf{I}) \mathbf{z}_{k+1} \quad (30c)$$

$$\mathbf{w}_{k+1} = -\tau (\mathbf{K} \otimes \mathbf{I}) \mathbf{y}_{k+1} \quad (30d)$$

$$\mathbf{e}_{k+1} = \nabla_{\mathbf{x}} \mathcal{L}_k(\mathbf{x}_{k+1}, \mathbf{w}_{k+1}) \quad (30e)$$

$$\mathbf{f}_{k+1} = \nabla_{\mathbf{w}} \mathcal{L}_k(\mathbf{x}_{k+1}, \mathbf{w}_{k+1}) \quad (30f)$$

where the matrices \mathbf{F} , \mathbf{C} and \mathbf{K} are defined in (27) and $\mathbf{z}_k \in \mathbb{R}^{nm}$, $\mathbf{y}_k \in \mathbb{R}^{pm}$ are the state vectors of the controller. Hence, equations (30) describe the online algorithm in the scheme of Figure 1.

3.5 Convergence

In this section we prove the convergence of Algorithm (30) solving the optimization problem described in (7). Convergence is established by the following proposition, which employs classical arguments based on a \mathcal{Z} -transforms.

Proposition 10 (Convergence of Algorithm 30)

Consider the optimization problem (7), with $\{\mathbf{b}_k\}_{k \in \mathbb{N}}$ and $\{\mathbf{h}_k\}_{k \in \mathbb{N}}$ modeled by (8). Choose the controller (17) with τ satisfying (23) and let $c(z)$ be such that $\mathbf{F}_c(\lambda)$, defined in (27), is asymptotically stable for all $\lambda \in [\tau\lambda(\mathbf{G}\mathbf{A}^{-1}\mathbf{G}^\top), \bar{\lambda}(\mathbf{A})]$. Let $\{\mathbf{x}_k\}_{k \in \mathbb{N}}$ be the output of the online algorithm (30). Then it holds

$$\limsup_{k \rightarrow \infty} \|\mathbf{x}_k - \mathbf{x}_k^*\| = 0.$$

PROOF. For the proof we follow the reasoning of [3, Proposition 1]. Given the control structure (17) and considering that interval $[\tau\lambda(\mathbf{G}\mathbf{A}^{-1}\mathbf{G}^\top), \bar{\lambda}(\mathbf{A})]$ includes the interval $[\lambda(\tilde{\mathcal{A}}(\tau)), \bar{\lambda}(\tilde{\mathcal{A}}(\tau))]$, selecting a controller $c(z)$ that stabilizes the matrix $\mathbf{F}_c(\lambda)$ for $\lambda \in [\tau\lambda(\mathbf{G}\mathbf{A}^{-1}\mathbf{G}^\top), \bar{\lambda}(\mathbf{A})]$ ensures the asymptotic stability of the poles of $\hat{\mathbf{e}}(z)$ and of $\hat{\mathbf{f}}(z)$, cf. (16). Consequently, the gradient of the Lagrangian, given by \mathbf{e}_k , \mathbf{f}_k , converges to zero, and this implies the thesis. \square

Remark 11 When the cost function f_k is not quadratic and the constraints are time varying, the convergence to zero of tracking error is not guaranteed. Similarly to what has been done in [3], in this case one can apply techniques based on the small gain theorem to establish bounds on this error. We opt against presenting this analysis here due to its significant intricacy. Furthermore, its results yield relatively broad bounds in comparison to what is shown by numerical experiments. As a result, we find it more suitable to substantiate the algorithm's good performance in addressing general online optimization problems only through the evidence presented by numerical experiments, which will be proposed in Section 5.

4 Online Optimization with Equality and Inequality Constraints

In this section, we aim to extend the previous approach to also handle linear inequality constraints.

4.1 Problem formulation

Consider now Problem (2) where we assume that the signal \mathbf{h}'_k has a rational \mathcal{Z} -transform, given by

$$\hat{\mathbf{h}}'(z) := \mathcal{Z}[\mathbf{h}'_k] = \frac{\mathbf{h}'_N(z)}{p(z)} \quad (31)$$

A commonly employed approach to address this problem is to extend the *primal-dual* algorithm to the *projected primal-dual* [7,8], which yields

$$\begin{aligned} \mathbf{x}_{k+1} &= \mathbf{x}_k - \alpha \nabla_{\mathbf{x}_k} \mathcal{L}'_k(\mathbf{x}_k, \mathbf{w}_k, \mathbf{w}'_k), \\ \mathbf{w}_{k+1} &= \mathbf{w}_k + \beta \nabla_{\mathbf{w}_k} \mathcal{L}'_k(\mathbf{x}_k, \mathbf{w}_k, \mathbf{w}'_k), \\ \mathbf{w}'_{k+1} &= \text{proj}_{\geq 0} \left(\mathbf{w}'_k + \gamma \nabla_{\mathbf{w}'_k} \mathcal{L}'_k(\mathbf{x}_k, \mathbf{w}_k, \mathbf{w}'_k) \right). \end{aligned} \quad (32)$$

Here, α , β , and γ are positive parameters, $\mathbf{w}_k \in \mathbb{R}^p$ and $\mathbf{w}'_k \in \mathbb{R}^{p'}$ are the Lagrange multipliers associated with the equality and the inequality constraints and \mathcal{L}'_k is the time-varying Lagrangian defined as

$$\mathcal{L}'_k(\mathbf{x}, \mathbf{w}, \mathbf{w}') := f_k(\mathbf{x}) + \mathbf{w}^\top (\mathbf{G}\mathbf{x} - \mathbf{h}_k) + \mathbf{w}'^\top (\mathbf{G}'\mathbf{x} - \mathbf{h}'_k).$$

The main difference between Algorithms (12) and (32) is the presence of a projection in the update of the dual variable associated with the inequality constraints. This projection works as a saturation to zero of the negative entries of the signal.

The first attempt in the design of an online optimization algorithm based on the Internal Model principle is simply applying what we did in the case in which we have only equality constraints. Precisely, we determine the controller using the internal model $p(z)$ as done in the previous section, considering inequality constraints as they were further equality constraints, and we incorporate in the resulting algorithm the saturation as done in (32). However, if we do this, we observe in the experiments the output of the proposed algorithm achieves very poor tracking, worse than the unstructured online primal-dual algorithm. Indeed, it is well-known that a controller based on the internal model with marginally unstable poles, coupled with a saturation, gives rise to significant transient phenomena known as wind-up. In order to mitigate this negative effect of the saturation, an anti wind-up mechanism, called back-calculation [1], is added to the algorithm. The resulting algorithm is

illustrated in Figure 2 and described by the following equations (33)

$$\mathbf{z}_{k+1} = (\mathbf{F} \otimes \mathbf{I}) \mathbf{z}_k + (\mathbf{C} \otimes \mathbf{I}) \mathbf{e}_k \quad (33a)$$

$$\mathbf{y}_{k+1} = (\mathbf{F} \otimes \mathbf{I}) \mathbf{y}_k + (\mathbf{C} \otimes \mathbf{I}) \mathbf{f}_k \quad (33b)$$

$$\mathbf{y}'_{k+1} = (\mathbf{F} \otimes \mathbf{I}) \mathbf{y}'_k + (\mathbf{C} \otimes \mathbf{I}) \mathbf{f}'_k \quad (33c)$$

$$\mathbf{x}_{k+1} = (\mathbf{K} \otimes \mathbf{I}) \mathbf{z}_{k+1} \quad (33d)$$

$$\mathbf{w}_{k+1} = -\tau (\mathbf{K} \otimes \mathbf{I}) \mathbf{y}_{k+1} \quad (33e)$$

$$\mathbf{v}_{k+1} = -\tau (\mathbf{K} \otimes \mathbf{I}) \mathbf{y}'_{k+1} \quad (33f)$$

$$\mathbf{w}'_{k+1} = \text{proj}_{\geq 0}(\mathbf{v}_{k+1}) \quad (33g)$$

$$\mathbf{e}_{k+1} = \nabla_{\mathbf{x}} \mathcal{L}'_{k+1}(\mathbf{x}_{k+1}, \mathbf{w}_{k+1}, \mathbf{w}'_{k+1}) \quad (33h)$$

$$\mathbf{f}_{k+1} = \nabla_{\mathbf{w}} \mathcal{L}'_{k+1}(\mathbf{x}_{k+1}, \mathbf{w}_{k+1}, \mathbf{w}'_{k+1}) \quad (33i)$$

$$\mathbf{f}'_{k+1} = \nabla_{\mathbf{w}'} \mathcal{L}'_{k+1}(\mathbf{x}_{k+1}, \mathbf{w}_{k+1}, \mathbf{w}'_{k+1}) + \underbrace{\rho (\mathbf{w}'_{k+1} - \mathbf{v}_{k+1})}_{\text{antiwind-up}}. \quad (33j)$$

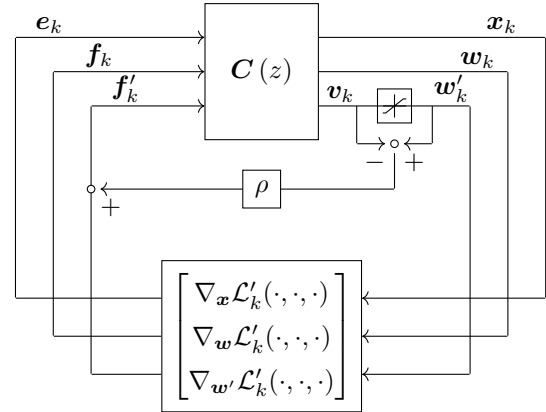


Fig. 2. The control scheme designed to solve (2).

where ρ is a positive tunable anti wind-up parameter, the matrices \mathbf{F} , \mathbf{C} and \mathbf{K} are defined in (27) and $\mathbf{z}_k \in \mathbb{R}^{nm}$, $\mathbf{y}_k \in \mathbb{R}^{pm}$, $\mathbf{y}'_k \in \mathbb{R}^{p'm}$ are the state vectors of the controller.

We are not able at present to give proofs of the convergence of this algorithm whose performance will be analysed only by means of numerical experiments.

5 Numerical Experiments

In this section we compare the performance of the different proposed algorithms when applied to the Problem (7) and to the Problem (2). In addition to addressing Problem (7), we also provide a numerical example to demonstrate that the algorithm performs well even

when the matrices \mathbf{A} and \mathbf{G} are time-varying and in more general non-quadratic cases.

5.1 Equality constraints

First we consider Problem (7) with $\mathbf{x} \in \mathbb{R}^n$, where $n = 10$. The matrix \mathbf{A} is defined as $\mathbf{A} = \mathbf{V}\mathbf{\Lambda}\mathbf{V}^\top$, where \mathbf{V} is a randomly generated orthogonal matrix, and $\mathbf{\Lambda}$ is a diagonal matrix with elements in the range $[1, 10]$. On the other hand, $\mathbf{G} \in \mathbb{R}^{p \times n}$ is a randomly generated matrix with orthogonal rows.

For the linear terms $\{\mathbf{b}_k\}_{k \in \mathbb{N}}$ and $\{\mathbf{h}_k\}_{k \in \mathbb{N}}$, we used the following models:

- (1) Triangular wave (Figure 3): $\mathbf{b}_k = \text{triang}(\omega k) \mathbf{1}$, $\mathbf{h}_k = \text{triang}(\omega k) \mathbf{1}$ with $\omega = 10^{-4}\pi$;
- (2) Sine: $\mathbf{b}_k = \sin(\omega k) \mathbf{1}$, $\mathbf{h}_k = \sin(\omega k) \mathbf{1}$ with $\omega = 10^{-4}\pi$.

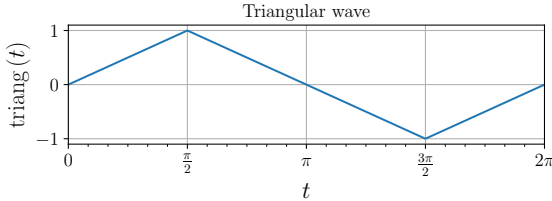


Fig. 3. The graph of the $\text{triang}(t) := 4 \left| \frac{t}{2\pi} - \lfloor \frac{t}{2\pi} + 3/4 \rfloor + 1/4 \right| - 1$, $t \in \mathbb{R}$.

In Figure 4, we compare our algorithm, based on a control approach, with $p(z) = z^2 - 2 \cos(\omega)z + 1$ for the sine and with the double integrator $p(z) = (z - 1)^2$ for the triangular wave, with the standard *primal-dual* (12) algorithm. From a control perspective, the classical *primal-dual* algorithm can be seen as a controller with only an integrator as internal model. Therefore, for example, when considering the sine, the controller is unable to guarantee perfect tracking but only tracking with a bounded error. On the other hand, the control approach design based on the correct model is capable of guaranteeing perfect tracking. In the case of the triangular wave, we can see that the Internal Model principle is piece-wise verified and then the tracking is always guaranteed except when there is a change of the slope in the signal. In these time instants a transient is required by the controller in order to track back the reference.

5.2 Inequality constraints

In this section, we consider Problem (2) with only inequality constraints, and we compare three different approaches to solve this optimization problem. In the simulations we set $n = 10$ and we use the same matrix \mathbf{A} used in Example 5.1 and as \mathbf{G}' we take the matrix \mathbf{G}

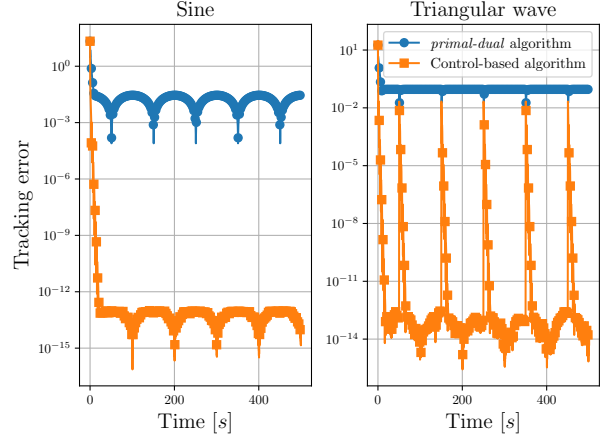


Fig. 4. Comparison between the *primal-dual* and the control-based algorithm in a semilogarithmic plot in case of sinusoidal or triangular wave signals.

used in Example 5.1. The signals \mathbf{b}_k and \mathbf{h}'_k are triangular waves with a periodicity of $\omega = 10^{-4}\pi$ and we take as model the double integrator.

In Figure 5, we compare three different algorithms:

- *Projected primal-dual* algorithm: This is the classical Algorithm (32) used in both Figure 4 and Figure 5 as the baseline method.
- Control-based algorithm modification of Equations (30), which includes the saturation block but with $\rho = 0$, so that it does not incorporate the anti wind-up mechanism shown in Figure 2.
- Control-based approach with anti wind-up compensation and $\rho = 1$ presented in Equations (33) and realized in the control scheme depicted in Figure 2.

To compare the tracking performance of the three different algorithms, we separate the analysis into two time windows separating the case in which the inequality constraint is active or inactive. In other words, if we denote \mathbf{x}_k^* the optimal solution with inequality constraints and $\mathbf{x}_{k,\text{UNC}}^*$ the optimal solution without inequality constraints, we analyse what happens for the k 's when $\mathbf{x}_k^* = \mathbf{x}_{k,\text{UNC}}^*$ and when $\mathbf{x}_k^* \neq \mathbf{x}_{k,\text{UNC}}^*$.

When k is such that $\mathbf{x}_k^* = \mathbf{x}_{k,\text{UNC}}^*$ and assuming that Equations (33) converge to the optimal couple $(\mathbf{x}_k, \mathbf{w}_k) \rightarrow (\mathbf{x}_k^*, \mathbf{w}_k^*)$ as k increases, we observe that both the control-based algorithm with and without anti wind-up have the dual variable $\mathbf{w}'_k = 0$, thanks to the complementary slackness condition [7]. Then, dynamics (33a) is decoupled by (33c) and the algorithm does not utilize the dual variable \mathbf{w}'_k in computing the optimum. Therefore, Equations (30) and (33) are practically equivalent, as we can see also from Figure 5. Nevertheless, the error \mathbf{f}'_k in Equation (33k), and consequently \mathbf{y}'_k in Equation (33c), are always influenced

by the gradient $\nabla_{\mathbf{w}'} \mathcal{L}'_k(\mathbf{x}_k, \mathbf{w}'_k)$, even if $\mathbf{w}'_k = 0$ and \mathbf{x}_k is approaching the true optimum. From a control perspective, this is the main effect of the wind-up: certain internal state variables of the controller (in this case \mathbf{y}'_k) continue to accumulate error even when the desired set point is reached. Hence, the absence of anti wind-up does not lead to a degradation of performance in these regions of Figure 5, actually the internal variable of the controller associated with the dual variable keeps growing, but it is not affecting the primal variable.

When k is such that $\mathbf{x}_k^* \neq \mathbf{x}_{k, \text{UNC}}^*$, namely the true optimum lies on the region where the linear inequality constraints in Problem (2) are violated, the inequality constraints act as equality constraints. Then the true optimum is identified by a couple $(\mathbf{x}_k^*, \mathbf{w}'_k^*)$ with $\mathbf{w}'_k^* \neq 0$ and once \mathbf{w}'_k becomes different from zero Equation (33g) becomes an identity map, making Algorithm (30) and Algorithm (33) identical. As discussed earlier, the control-based algorithm guarantees perfect tracking. However, as shown in Figure 5, there is a significant difference between the two Algorithms when passing through the red region. This difference is due to the wind-up that results in a delay of \mathbf{w}'_k relative to \mathbf{w}'_k^* in going from $\mathbf{w}'_k = 0$ to $\mathbf{w}'_k \neq 0$.

The main issue arises when the dual variable \mathbf{w}'_k becomes saturated. In such cases, the algorithm continues to integrate the error \mathbf{f}'_k and increases the internal state variables associated with the integral actions. Ideally, when saturation is active, we are within the bounds of the inequality constraints, allowing the optimization algorithm to work as an unconstrained optimization. Consequently, the integration of the error \mathbf{f}'_k becomes not only redundant but also detrimental. The integral actions retain memory of the previously integrated error and negatively affect the algorithm's performance even outside the saturation region. The anti wind-up mechanism aims to reduce these integral actions when they are unnecessary, attempting to directly compensate for the input \mathbf{f}'_k .

Finally, in Figure 5 we can see the presence of some transient effects, some related to the crossing of the red region the others linked to the change of the slope in the triangular wave.

5.3 Time-varying quadratic term and constraint

As done in [3], to assess the performance of our algorithm in more complex scenarios, we undertake an experimental validation. In these experiments we take $n = 10$ and $p = 2$. This begins by considering a time-varying quadratic term $\mathbf{A}_k = \mathbf{A}_1 + \sin(\omega k) \mathbf{A}_2$, where \mathbf{A}_1 is symmetric positive definite and with eigenvalues within the interval $[1, 10]$, \mathbf{A}_2 is a symmetric sparse matrix of ones, where, the non zeros elements are in the ten percent of

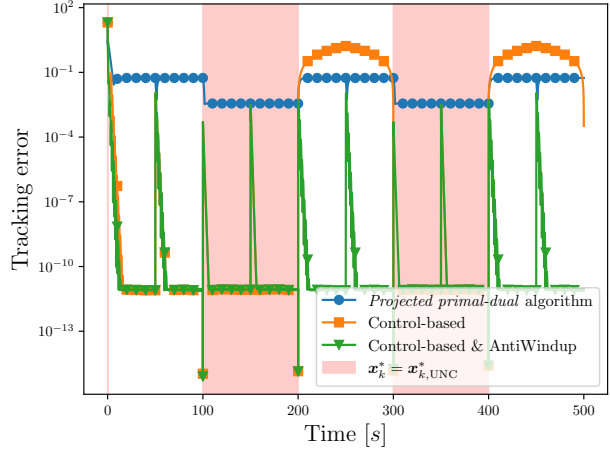


Fig. 5. Comparison between the *projected primal-dual*, the control-based without anti wind-up, and the control-based with anti wind-up compensation in a semilogarithmic plot where \mathbf{b}_k and \mathbf{h}'_k are assumed to be two triangular waves.

its entries. Moreover, we also consider time-varying constraints. Precisely, we set $\mathbf{G}_k = \mathbf{G}_1 + \sin(\omega k) \mathbf{G}_2$ where \mathbf{G}_1 is a random rectangular matrix with singular values in the range $[1, 3]$ and, similar as before, \mathbf{G}_2 is a sparse matrix with the ten percent of its entries that are ones. The sinusoidal term $\sin(\omega k)$ has $\omega = 1/2$. The remaining terms in Problem (7) are held constant, namely $\mathbf{b}_k = \bar{\mathbf{b}} \in \mathbb{R}^n$ and $\mathbf{h}_k = \bar{\mathbf{h}} \in \mathbb{R}^p$.

To implement our Algorithm we require an internal model that captures the dynamic nature of $f_k(\mathbf{x})$. In view of the periodic evolution of $f_k(\mathbf{x})$, reasonable choices of the internal model are

$$p(z) = (z - 1) \prod_{l=1}^L [z^2 - 2 \cos(l\omega) z + 1], \quad L \in \mathbb{N}. \quad (34)$$

Since $f_k(\mathbf{x})$ is non-linear, we can only approximate the internal model. Utilizing model (34), we aim to capture the model's minimum periodicity and fast variations.

The results of these simulations are depicted in Figure 6. As we can see, Algorithm (30) exhibits better performance than the *primal-dual* algorithm. Moreover, taking more complex internal models, we can improve the performance on the tracking error at the cost of a slower convergence rate. This slower convergence is characteristic of the internal model principle, as the controller requires a certain amount of time to reach its steady state response. This duration increases with the complexity of the internal model. Nevertheless, given our primary interest in the algorithm's asymptotic performances, this trade-off can be considered acceptable.

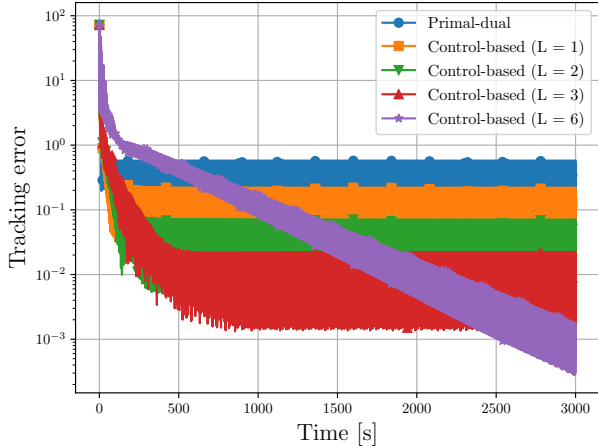


Fig. 6. Comparison between the *primal-dual* algorithm, and the control-based with models of Equation (34) ($L = 1, 2, 3, 6$) in the time-varying case.

5.4 Non-quadratic cost

In this section, we present an additional example of the application of our algorithm in a setting where the objective function is non-quadratic. Specifically, we utilize the following function taken from [36]

$$f_k(\mathbf{x}) = \frac{1}{2} \mathbf{x}^\top \mathbf{A} \mathbf{x} + \mathbf{b}^\top \mathbf{x} + \sin(\omega k) \log [1 + \exp(\mathbf{c}^\top \mathbf{x})],$$

subject to the constraint:

$$\mathbf{G} \mathbf{x} = \mathbf{h}_k.$$

In the above equations we take $\omega = 1/2$, $n = 10$, $\mathbf{b}, \mathbf{c} \in \mathbb{R}^n$ with \mathbf{c} such that $\|\mathbf{c}\| = 1$. The matrix $\mathbf{A} \in \mathbb{R}^{n \times n}$ and $\mathbf{G} \in \mathbb{R}^{p \times n}$, with $p = 1$, are generated as described in Section 5.1, and the term \mathbf{h}_k is the same as in case 2 of Section 5.1. Finally, in Figure 7, we report the tracking performance of the *primal-dual* algorithm along with three different versions of the control-based algorithm that implement the internal models of Equation (34). From Figure 7, we can see that the control-based method outperforms the *primal-dual* algorithm in terms of tracking performance, even if with a slower convergence rate.

6 Conclusions

In this paper we addressed the solution of online, constrained problems by leveraging control theory to design novel algorithms. When only equality constraints are present, we showed how to reformulate the problem as a robust, linear control problem, and we designed a suitable controller to achieve zero tracking error. When also inequality constraints are imposed, we showed how the required nonnegativity of the dual variables can lead

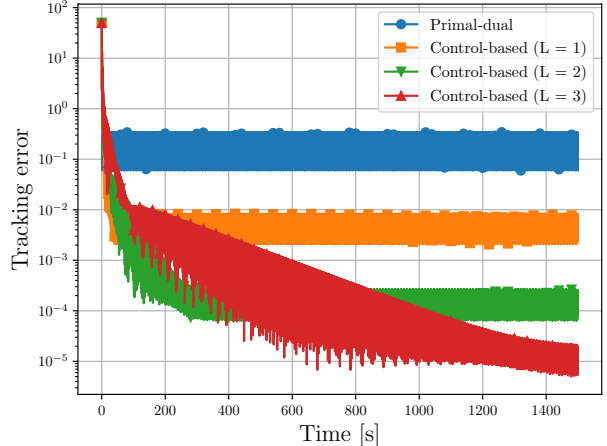


Fig. 7. Comparison between the *primal-dual* algorithm, and the control-based with models of Equation (34) ($L = 1, 2, 3$) in the non-quadratic case.

to a wind-up phenomenon. As a consequence, we propose a modified version of the algorithm that incorporates an anti-windup scheme. Overall, we showed with both theoretical and numerical results how the proposed approaches outperform state-of-the-art alternatives.

References

- [1] Karl Johan Astrom and Lars Rundqwist. Integrator windup and how to avoid it. In *1989 American Control Conference*, pages 1693–1698. IEEE, 1989.
- [2] Nicola Bastianello, Ruggero Carli, and Andrea Simonetto. Extrapolation-Based Prediction-Correction Methods for Time-varying Convex Optimization. *Signal Processing*, 210:109089, 2023.
- [3] Nicola Bastianello, Ruggero Carli, and Sandro Zampieri. Internal Model-Based Online Optimization. *IEEE Transactions on Automatic Control*, pages 1–8, 2023.
- [4] Michele Benzi, Gene H. Golub, and Jörg Liesen. Numerical solution of saddle point problems. *Acta Numerica*, 14:1–137, May 2005.
- [5] Michele Benzi and Valeria Simoncini. On the eigenvalues of a class of saddle point matrices. *Numerische Mathematik*, 103(2):173–196, April 2006.
- [6] Andrey Bernstein, Emiliano Dall’Anese, and Andrea Simonetto. Online Primal-Dual Methods With Measurement Feedback for Time-Varying Convex Optimization. *IEEE Transactions on Signal Processing*, 67(8):1978–1991, April 2019.
- [7] Dimitri P Bertsekas. *Constrained optimization and Lagrange multiplier methods*. Academic press, 2014.
- [8] Stephen Boyd and Lieven Vandenberghe. *Convex Optimization*. Cambridge University Press, 2004.
- [9] Xuanyu Cao and K. J. Ray Liu. Online Convex Optimization With Time-Varying Constraints and Bandit Feedback. *IEEE Transactions on Automatic Control*, 64(7):2665–2680, July 2019.
- [10] Tsung-Hui Chang, Mingyi Hong, Hoi-To Wai, Xinwei Zhang, and Songtao Lu. Distributed Learning in the Nonconvex

- World: From batch data to streaming and beyond. *IEEE Signal Processing Magazine*, 37(3):26–38, May 2020.
- [11] Marcello Colombino, Emiliano Dall’Anese, and Andrey Bernstein. Online Optimization as a Feedback Controller: Stability and Tracking. *IEEE Transactions on Control of Network Systems*, 7(1):422–432, March 2020.
- [12] Emiliano Dall’Anese, Andrea Simonetto, Stephen Becker, and Liam Madden. Optimization and Learning With Information Streams: Time-varying algorithms and applications. *IEEE Signal Processing Magazine*, 37(3):71–83, May 2020.
- [13] Alexander Davydov, Veronica Centorrino, Anand Gokhale, Giovanni Russo, and Francesco Bullo. Contracting Dynamics for Time-Varying Convex Optimization, May 2023. arXiv:2305.15595 [cs, eess, math].
- [14] M.C. de Oliveira, J. Bernussou, and J.C. Geromel. A new discrete-time robust stability condition. *Systems & Control Letters*, 37(4):261–265, July 1999.
- [15] Rishabh Dixit, Amrit Singh Bedi, Ruchi Tripathi, and Ketan Rajawat. Online Learning with Inexact Proximal Online Gradient Descent Algorithms. *IEEE Transactions on Signal Processing*, 67(5):1338 – 1352, 2019.
- [16] Mahyar Fazlyab, Santiago Paternain, Victor M. Preciado, and Alejandro Ribeiro. Prediction-Correction Interior-Point Method for Time-Varying Convex Optimization. *IEEE Transactions on Automatic Control*, 63(7):1973–1986, July 2018.
- [17] Sophie M. Fosson. Centralized and Distributed Online Learning for Sparse Time-Varying Optimization. *IEEE Transactions on Automatic Control*, 66(6):2542–2557, June 2021.
- [18] Guilherme França, Daniel P. Robinson, and René Vidal. Gradient flows and proximal splitting methods: A unified view on accelerated and stochastic optimization. *Physical Review E*, 103(5):053304, May 2021.
- [19] Eric C. Hall and Rebecca M. Willett. Online Convex Optimization in Dynamic Environments. *IEEE Journal of Selected Topics in Signal Processing*, 9(4):647–662, June 2015.
- [20] Adrian Hauswirth, Saverio Bolognani, Gabriela Hug, and Florian Dorfler. Timescale Separation in Autonomous Optimization. *IEEE Transactions on Automatic Control*, 66(2):611–624, 2021.
- [21] Laurent Lessard, Benjamin Recht, and Andrew Packard. Analysis and Design of Optimization Algorithms via Integral Quadratic Constraints. *SIAM Journal on Optimization*, 26(1):57–95, January 2016.
- [22] Yingying Li, Guannan Qu, and Na Li. Online Optimization With Predictions and Switching Costs: Fast Algorithms and the Fundamental Limit. *IEEE Transactions on Automatic Control*, 66(10):4761–4768, October 2021.
- [23] Dominic Liao-McPherson, Marco Nicotra, and Ilya Kolmanovskiy. A Semismooth Predictor Corrector Method for Real-Time Constrained Parametric Optimization with Applications in Model Predictive Control. In *2018 IEEE Conference on Decision and Control (CDC)*, pages 3600–3607, December 2018.
- [24] Alberto Natali, Mario Coutino, Elvin Isufi, and Geert Leus. Online Time-Varying Topology Identification Via Prediction-Correction Algorithms. In *ICASSP 2021 - 2021 IEEE International Conference on Acoustics, Speech and Signal Processing (ICASSP)*, pages 5400–5404, Toronto, ON, Canada, June 2021. IEEE.
- [25] S. Paternain, M. Morari, and A. Ribeiro. Real-Time Model Predictive Control Based on Prediction-Correction Algorithms. In *2019 IEEE 58th Conference on Decision and Control (CDC)*, pages 5285–5291, 2019.
- [26] Carsten Scherer and Christian Ebenbauer. Convex Synthesis of Accelerated Gradient Algorithms. *SIAM Journal on Control and Optimization*, 59(6):4615–4645, January 2021.
- [27] Carsten W. Scherer, Christian Ebenbauer, and Tobias Holicki. Optimization Algorithm Synthesis based on Integral Quadratic Constraints: A Tutorial, June 2023.
- [28] Daniel Selvaratnam, Iman Shames, Jonathan H Manton, and Mohammad Zamani. Numerical Optimisation of Time-Varying Strongly Convex Functions Subject to Time-Varying Constraints. In *2018 IEEE Conference on Decision and Control (CDC)*, pages 849–854, December 2018.
- [29] Shahin Shahrampour and Ali Jadbabaie. An online optimization approach for multi-agent tracking of dynamic parameters in the presence of adversarial noise. In *2017 American Control Conference (ACC)*, pages 3306–3311, 2017.
- [30] Shahin Shahrampour and Ali Jadbabaie. Distributed Online Optimization in Dynamic Environments Using Mirror Descent. *IEEE Transactions on Automatic Control*, 63(3):714–725, March 2018.
- [31] Shai Shalev-Shwartz. Online Learning and Online Convex Optimization. *Foundations and Trends® in Machine Learning*, 4(2):107–194, 2011.
- [32] Shu-Qian Shen, Ting-Zhu Huang, and Juan Yu. Eigenvalue Estimates for Preconditioned Nonsymmetric Saddle Point Matrices. *SIAM Journal on Matrix Analysis and Applications*, 31(5):2453–2476, January 2010.
- [33] A. Simonetto, E. Dall’Anese, S. Paternain, G. Leus, and G. B. Giannakis. Time-Varying Convex Optimization: Time-Structured Algorithms and Applications. *Proceedings of the IEEE*, 108(11):2032–2048, November 2020.
- [34] Andrea Simonetto and Emiliano Dall’Anese. Prediction-Correction Algorithms for Time-Varying Constrained Optimization. *IEEE Transactions on Signal Processing*, 65(20):5481–5494, October 2017.
- [35] Andrea Simonetto and Paolo Massioni. Optimization Filters for Stochastic Time-Varying Convex Optimization. In *2023 European Control Conference (ECC)*, pages 1–6, 2023.
- [36] Andrea Simonetto, Aryan Mokhtari, Alec Koppel, Geert Leus, and Alejandro Ribeiro. A Class of Prediction-Correction Methods for Time-Varying Convex Optimization. *IEEE Transactions on Signal Processing*, 64(17):4576–4591, September 2016.
- [37] A. Sundararajan, B. Van Scoy, and L. Lessard. A Canonical Form for First-Order Distributed Optimization Algorithms. In *2019 American Control Conference (ACC)*, pages 4075–4080, July 2019.
- [38] Guodong Zhang, Xuchan Bao, Laurent Lessard, and Roger Grosse. A Unified Analysis of First-Order Methods for Smooth Games via Integral Quadratic Constraints. *Journal of Machine Learning Research*, 22(103):1–39, 2021.
- [39] Y. Zhang, E. Dall’Anese, and M. Hong. Online Proximal-ADMM for Time-Varying Constrained Convex Optimization. *IEEE Transactions on Signal and Information Processing over Networks*, 7:144–155, 2021.